Rational Resolution Decompositions for Signal Processing

Bruce P. Anderson

Department of Electrical Engineering
Air Force Institute of Technology
Wright Patterson AFB, OH 45433

Gregory T. Warhola

Department of Mathematics and Statistics
Air Force Institute of Technology
Wright Patterson AFB, OH 45433

1 Introduction

Dyadic multiresolution analyses (MRAs) and their relationships to quadrature-mirror filter banks is well known[2][3]. Recently, MRAs based on arbitrary integer dilation factors have been developed[1][4] and strong connections with M-channel perfect-reconstruction filter banks have been made[5]. In this paper we present the concept of a rational resolution analysis (RRA) which is similar to the M-dilation MRAs, except we allow M to be a positive *rational* number. The RRA is developed by relaxing the requirement that the successive approximation spaces be embedded. This requires a slightly more complicated scheme for reconstruction and it limits the choices of scaling functions and wavelets which can be used. For discrete-time signal processing, the RRA provides a rational sampling rate change with specific requirements imposed upon the anti-aliasing filter.

2 Rational Resolution Analysis

In a typical MRA with integer dilation factor M, a signal $f \in V_{m-1}$, a subspace of $L^2(\mathbb{R})$, is decomposed by projecting onto M orthogonal subspaces: one "approximation" space V_m and $M-1$ "detail" spaces W_m^k, $k = 1, 2, \ldots, M-1$. In practice, the signal f is represented by its coefficients with respect to a basis of V_{m-1} and the projections are implemented with fast discrete filters on those coefficients. The approximation spaces are embedded ($V_m \subset V_{m-1}$) and we have

$$f(\cdot) \in V_{m-1} \Longleftrightarrow f(\cdot/M) \in V_m. \tag{1}$$

Furthermore, there exists a scaling function $\phi \in V_0$ such that $\{{}_M\phi_{mn}\}_{n\in\mathbb{Z}}$ forms an orthonormal basis for V_m where ${}_M\phi_{mn}(t) = M^{-m/2}\phi(M^{-m}t - n)$. Hence, f is uniquely represented by its approximation coefficients defined by $c_{mn} = \langle f, {}_M\phi_{mn}\rangle$ where $\langle\cdot,\cdot\rangle$ is the standard $L^2(\mathbb{R})$ inner product. The approximation projection operator on coefficients is defined by

$$c_{ml} = \sum_n h_{n-Ml} c_{m-1,n} \tag{2}$$

where

$$h_n = \langle {}_M\phi_{1,0}\, , \, {}_M\phi_{0,n}\rangle. \tag{3}$$

The detail coefficients and projection operators are defined similarly by $d_{ml}^k = \sum_n g_{n-pl}^k c_{m-1,n}$ where $g_n = \langle {}_M\psi_{1,0}^k\, , \, {}_M\phi_{0,n}\rangle$ and $\{{}_M\psi_{mn}^k\}_{n\in\mathbb{Z}}$ (defined analogously to ${}_M\phi_{mn}$) forms an orthonormal basis for W_m^k.

An MRA decomposition successively projects the signal f from one approximation space to the next. At each step, the part of the signal lost in the approximation is captured in the detail spaces. Reconstruction is accomplished by a direct sum of all the projections. It is implemented again by working directly with the coefficients using discrete filter operations:

$$c_{m-1,n} = \sum_l h_{n-pl} c_{ml} + \sum_{k=1}^{p-1} \sum_l g_{n-pl}^k d_{ml}^k.$$

For a rational resolution analysis the dilation factor is $M = p/q$ where p and q are integers satisfying $p > q \geq 1$ and are mutually coprime. Adjacent approximation spaces are related as in (1) but with a rational dilation factor, the projection operators are more complicated. A signal $f \in V_0$ can be expanded $f(t) = \sum_n c_{0n}\ {}_{p/q}\phi_{0n}(t)$ and the first level approximation is given by $(P_1^{p/q} f)(t) = \sum_k c_{1k}\ {}_{p/q}\phi_{1k}(t)$. Expressing the $\{c_{1k}\}_{k\in\mathbb{Z}}$ in terms of the coefficients of the expansion of $f \in V_0$,

$$c_{1k} = \sum_n c_{0n} \langle {}_{p/q}\phi_{0n}, {}_{p/q}\phi_{1k}\rangle, \tag{4}$$

relates the two sets of approximation coefficients.

For an integer dilation, the relationship between the two sets of approximation coefficients is given in (3).

The approximation spaces are not embedded with a rational dilation factor[1] and so the relationship between adjacent sets of approximation coefficients is more complex. We express this relationship by defining a filter matrix $\mathbf{H}$ by $\mathbf{H}_{kn} = \langle {}_{p/q}\phi_{0n}\, , {}_{p/q}\phi_{1k}\rangle$, so that the approximation coefficients vectors, $\mathbf{c}_0$ and $\mathbf{c}_1$, satisfy $\mathbf{c}_1 = \mathbf{H}\mathbf{c}_0$. This development is valid for integer dilation factors except in that case the structure of $\mathbf{H}$ allows the simpler expressions of (3) and (2).

In either case, $\mathbf{H}$ will have a repeated block structure caused by the periodic behavior of the inner product:

$$\langle {}_{p/q}\phi_{1k}\, , {}_{p/q}\phi_{0n}\rangle = \langle {}_{p/q}\phi_{0,k-lq}\, , {}_{p/q}\phi_{1,n-lp}\rangle, \quad l \in \mathbb{Z}. \quad (5)$$

The dimensions of the block will depend on the rational dilation factor and the support of the scaling function. A block will have q distinct rows and will be offset from an adjacent block by p columns. Alternatively, a block will have p distinct columns with a row offset of q. These two interpretations are shown in Figure 1. Whether or not a compactly supported scaling function is used will determine whether the block is finite in extent. Figure 1 illustrates the compact support case.

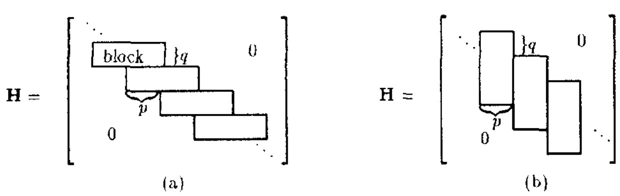

Figure 1: Block Structure of the Inner Product Matrix

The relationship between the approximation coefficients at adjacent levels can also be expressed in the frequency domain. By Parseval's relationship

$$\langle {}_{p/q}\phi_{0n}, {}_{p/q}\phi_{1k}\rangle = \langle \widehat{{}_{p/q}\phi_{0n}}, \widehat{{}_{p/q}\phi_{1k}}\rangle \quad (6)$$

where $\hat{\phi}$ is the Fourier transform of ϕ. With

$$\begin{aligned} \widehat{{}_{p/q}\phi_{0n}}(\omega) &= e^{-in\omega}\hat{\phi}(\omega), \\ \widehat{{}_{p/q}\phi_{1k}}(\omega) &= (p/q)^{1/2} e^{-i\frac{p}{q}k\omega}\hat{\phi}(\frac{p}{q}\omega), \end{aligned} \quad (7)$$

we have

$$\langle \widehat{{}_{p/q}\phi_{0n}}, \widehat{{}_{p/q}\phi_{1k}}\rangle = \frac{\sqrt{pq}}{2\pi}\int_{-\infty}^{\infty} \hat{\phi}(q\omega)\overline{\hat{\phi}(p\omega)} e^{i(nq-kp)\omega} d\omega. \quad (8)$$

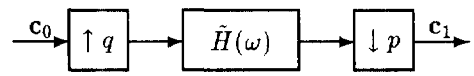

Figure 2: Filtering operation for the Rational Resolution Approximation

By defining $H(\omega) = \hat{\phi}(q\omega)\hat{\phi}(p\omega)$, (8) defines the inverse Fourier transform, h, of H so that $\langle {}_{p/q}\phi_{0n}, {}_{p/q}\phi_{1k}\rangle = h_{nq-kp}$. Defining $\tilde{H}(\omega) = \sum_n \tilde{h}_n e^{-in\omega}$, where $\tilde{h}_n = h_{-n}$, the operation $\mathbf{c}_1 = \mathbf{H}\mathbf{c}_0$ can be viewed as a filter operation where the $\{c_{0n}\}$ are upsampled by q, filtered with $\tilde{H}$, and downsampled by p (Figure 2). Substituting in (4) yields

$$c_{1k} = \sum_n c_{0n} h_{nq-kp}.$$

This is a well-known rational sampling rate change, except the lowpass filter is specifically chosen to relate the approximation coefficients at adjacent levels.

3 Rational Resolution Reconstruction

Like the decomposition, the reconstruction technique for the RRA is slightly more complex than the MRA. Embedded MRA approximation spaces allowed a signal to be decomposed into a component in the lower-resolution approximation space and a component in the detail space, which detail space may be generated by more than one wavelet. Since the detail space is the orthogonal complement of the approximation space with respect to the previous approximation space, the signal can be perfectly reconstructed by a direct sum of the two components.

With the RRA, V_m is not a subspace of V_{m-1} so it is impossible to form a detail space which is the orthogonal complement V_m in V_{m-1}. Hence, there are no wavelets which represent the detail information in the same way as the integer resolution wavelets so another scheme to recover the lost information must be considered.

Suppose $f \in V_{m-1}$ is projected onto V_m via a rational approximation operator $P^{p/q}$. Our goal is to reconstruct f from the approximated version $(P^{p/q}f)$. We first further approximate $(P^{p/q}f)$ by projecting it onto a space V'_m defined such that

$$V'_m = \overline{\text{span}\{D^{1/q}{}_{p/q}\phi_{ml}\}_{l\in\mathbf{Z}}}, \quad (9)$$

where D is defined as the dilation operator such that $(D^\theta f)(t) = f(\theta t)$. The $\{D^{1/q}{}_{p/q}\phi_{ml}\}_{l\in\mathbf{Z}}$ span the same space as the p-dilated basis functions of V_{m-1}. In other words, we also have

$$V'_m = \overline{\text{span}\{D^{1/p}{}_{p/q}\phi_{m-1,l}\}_{l\in\mathbf{Z}}}. \qquad (10)$$

Consequently, if ϕ is defined so that it satisfies the integer dilation equation $\hat{\phi}(p\omega) = H'(\omega)\hat{\phi}(\omega)$ for some $H'(\omega) = \sum_n h'(n)e^{-in\omega}$, it follows that we have $V'_m \subset V_{m-1}$. If V'_m is an embedded subspace of V_{m-1} based on an integer dilation factor of p, then it will have $p-1$ mutually orthogonal detail spaces as in an p-dilation MRA. From this point, the reconstruction is the same as an integer resolution analysis based on p. We define the following projection operators on $L^2(\mathbb{R})$:

$$\begin{aligned}
P_m^{p/q} f &= \sum_k \langle f, {}_{p/q}\phi_{mk}\rangle {}_{p/q}\phi_{mk}, \\
P_m^q f &= (1/q)\sum_l \langle f, D^{1/q}{}_{p/q}\phi_{ml}\rangle D^{1/q}{}_{p/q}\phi_{ml}, \\
P_m^p f &= (1/p)\sum_l \langle f, D^{1/p}{}_{p/q}\phi_{m-1,l}\rangle D^{1/p}{}_{p/q}\phi_{m-1,l}, \\
Q_m^p f &= \sum_l \langle f, D^{1/p}{}_{p/q}\psi_{m-1,l}\rangle D^{1/p}{}_{p/q}\psi_{m-1,l}. \qquad (11)
\end{aligned}$$

By the notation $D^{1/p}{}_{p/q}\psi_{m-1,l}$, we denote the wavelets which form the basis for the orthogonal complement of V'_m in V_{m-1}. The RRA approximation and reconstruction scheme is illustrated in Figure 3.

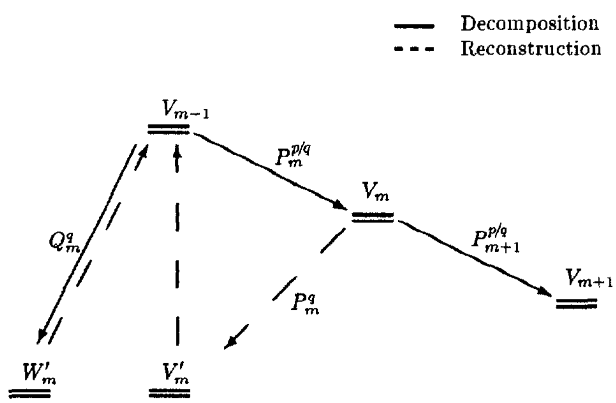

Figure 3: Summary of Rational Resolution Approximation and Reconstruction

Perfect reconstruction is not possible unless we start with the correct approximation in V'_m. So, we study the projection from V_m to V'_m. The projection onto V'_m must be the same regardless whether we project from V_{m-1} or V_m. This implies that for $f \in V_m$ we must have $P_m^q P_m^{p/q} f = P_m^p f$ which is equivalent to

$$D^{1/q}{}_{p/q}\phi_{ml} = \sum_k \langle {}_{p/q}\phi_{mk}, D^{1/q}{}_{p/q}\phi_{ml}\rangle {}_{p/q}\phi_{mk}. \qquad (12)$$

This simply says $D^{1/p}{}_{p/q}\phi_{ml}$ is a linear combination of the $D^{1/q}{}_{p/q}\phi_{mk}$, from which it follows that these spaces must also be embedded. Hence, perfect reconstruction implies $V'_m \subset V_{m-1}$ and $V'_m \subset V_m$. Dilating both sides (12) by $(p/q)^m$ gives

$${}_q\phi_{1l} = \sum_k \langle {}_{p/q}\phi_{1k}, {}_p\phi_{1l}\rangle \phi_{0k}. \qquad (13)$$

By substituting $\langle {}_{p/q}\phi_{mk}, D^{1/q}{}_{p/q}\phi_{ml}\rangle = \sqrt{q}\langle \phi_{0k}, {}_q\phi_{1l}\rangle$ in this expression, we arrive at the condition:

$${}_q\phi_{1l} = \sum_k \langle \phi_{0k}, {}_q\phi_{1l}\rangle \phi_{0k}. \qquad (14)$$

which implies the approximation operator which projects from V_m to V'_m is based on an integer dilation factor of q. That is, given a function $f \in V_m$, we have $P^q f \in V'_m$. This is significant because integer-based projection operations are generally easier to implement than rational ones.

4 Scaling functions and Perfect Reconstruction

For perfect reconstruction, the choice of scaling function plays a key role in the rational resolution analysis. The scaling functions are intrinsically related to the approximation spaces. Thus, placing requirements on the approximation spaces will influence the choice of scaling functions.

We want to show by example that the usual compactly-supported scaling functions[2, 1, 4] do not satisfy the perfect reconstruction scheme of the previous section. To do this, consider Equation 14 again. Suppose we are using a compactly supported scaling function based on an integer p dilation. We can calculate the sum in Equation 14, dilate it by $1/q$, and compare it to the original scaling function. Consider the following example.

Using the $p = 3$ compactly supported scaling function with 2 degrees of regularity (Figure 4 in [4]). Define the approximation space V_0 to be the span of its orthonormal integer translates. Now suppose $q = 2$. With $p = 3$, we calculate the inner products required in Equation 14. If this equation holds, then the scaling function dilated by 2 is in V_0. Conversely, ϕ_{00}

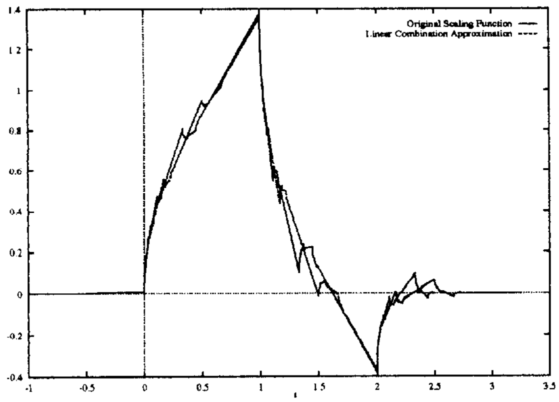

Figure 4: Comparison of $M = p = 3$ Compactly Supported Scaling Function[1][4] with Linear Combination of q-Dilated Scaling Functions.

should be in the space spanned by $D^2\phi_{0n}$ for $n \in \mathbb{Z}$. In Figure 4, we graphically compare ϕ_{00} and its projection onto the space spanned by of $D^2\phi_{0n}$ for $n \in \mathbb{Z}$. Although the two scaling functions have the same basic shape, they are not equal pointwise; they have unequal supports. From this we conclude that the approximation spaces V_m and V'_m are not embedded.

Because the approximation spaces based on compactly-supported scaling functions are not embedded, we cannot hope to obtain perfect reconstruction. However, because the shapes of the two scaling functions in the previous example are similar, we can expect a reasonable reconstruction. In order to see this effect of this approximation, we return to approximation coefficients and discrete filter operations.

The multiresolution analysis, rational or otherwise, is a linear transformation. As with most discrete linear systems, the impulse response is very important in that it provides a great deal of information about the characteristics of the system. The rational resolution approximation will generally have more than one impulse response. For simplicity, we demonstrate only one of three in the following example. Suppose we have a sequence of approximation coefficients $c_{0n} = \delta(n)$, the Kronecker delta function, which we want to decompose and reconstruct with RRA. Assume that $p = 3$ and $q = 2$ and the scaling function associated with the analysis is the one given in the previous example (Figure 4 in [4]). We decompose this set of approximation coefficients using the filter coefficients in Table 1 which are the numerically calculated inner products.

n	$h(n)$
-4	-0.000287420672395512
-3	-0.0440663791657491
-2	0.00572865007567187
-1	0.305000213846163
0	0.734891371897753
1	0.908269395408422
2	0.582716289665621
3	0.126436376018966
4	-0.0975392317518494
5	-0.0709325019117585
6	-0.000764787823073089
7	3.77671951090657e-05

Table 1: Rational Approximation Filter Coefficients

Now, the c_{1k} are filtered as in Equation 14. The resulting coefficients are approximate coefficients and we denote them by $\tilde{c}'_{1l}$.

The true approximation coefficients, c'_{1l}, are found by filtering the c_{0n} with the $M = p$ integer-resolution approximation filter. Reconstructing with the $\tilde{c}'_{1l}$ we obtain $\tilde{c}_{0n}$ which is an approximation of the original c_{0n} (relative l^2 error 4.12%). The $\tilde{c}_{0n}$ are given in Table 2. The impulse response is non-causal (has nonzero values for $n < 0$) because the filters used to obtain it are non-causal. In practice, we would be constrained to causal filters and would naturally expect a delay in the impulse response.

A requirement for perfect reconstruction is that the approximation spaces be embedded ($V'_m \subset V_m$). In this paper the approximation spaces were determined by the choice of scaling functions which were known *a priori*. Perfect reconstruction can be obtained by first defining the approximation spaces, then determining the corresponding scaling functions. Examples with embedded spaces are the spaces of spline functions which have their knots at the integers. The corresponding scaling functions can be found via the orthonormalization trick of Daubechies[2]. Since these spaces have knots at the integers, integer dilations are naturally embedded.

5 Fourier Domain Interpretation

Like the MRA, the RRA is implemented by discrete-time filter operations. For a p-dilation MRA, approximation is a low-pass filtering operation. The bandwidth of each successive approximation is roughly

n	$\tilde{c}_{0n}$
-9	2.198147937372851e-07
-8	3.448299084782647e-07
-7	4.698450232192443e-07
-6	-0.00578283042412773
-5	-0.009071908848033937
-4	-0.01236098727194014
-3	0.007340162900056513
-2	0.0171263011937004
-1	0.02691243948734121
0	1.002567516653402
1	-0.00705767970676463
2	-0.01668287606694384
3	-0.004025304999031559
4	-0.0009776385395248652
5	0.002070027919981815
6	-9.976394502917046e-05
7	-1.941892920712597e-05
8	6.092608661491856e-05

Table 2: Impulse Response Approximation Coefficients for a Rational Resolution Reconstruction

$1/p$ times that of the previous approximation. The details corresponding to a particular approximation contain the high frequency portions of the spectrum. The $p-1$ detail spaces contain the upper fraction $(1-1/p)$ of the spectrum of the previous approximation. For the RRA, the bandwidth of each successive approximation is roughly q/p times that of the previous approximation. The effective frequency response of the RRA approximation operation using the filter of the previous example is shown in Figure 5. The slow decay of the filters response is due to the low regularity of the scaling functions.

There are still $p-1$ detail spaces which contain the high frequency portions of the previous approximation. To use this information for reconstruction, the q/p approximation is further approximated by a factor of $1/q$ via another lowpass filter with a $1/q$ approximate bandwidth. The result is a bandlimited signal which contains the lower $1/p$ of the original signal. This yields the lowpass frequencies in a band of width $1/p$ times that of the spectrum being reconstructed.

6 Conclusion

This paper has introduced the rational resolution analysis which is a generalization of integer-dilation multiresolution analysis. The dilation factor is not

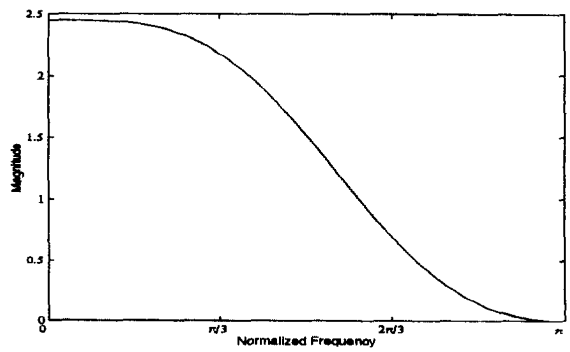

Figure 5: Effective frequency response for rational approximation filter (Table 1)

limited to the integers. We have demonstrated an example using the usual compactly supported scaling functions which do not lead to perfect reconstruction but for which the approximate reconstruction does not have large errors.

References

[1] Bruce P. Anderson. Theory and implementation of wavelet analyses in rational resolution decompositions. Master's thesis, Air Force Institute of Technology, Wright-Patterson AFB, Ohio 45433, 1992.

[2] Ingrid Daubechies. *Ten Lectures on Wavelets.* Society of Industrial and Applied Mathematics, 1992.

[3] Stephane G. Mallat. Multifrequency channel decompositions of images and wavelet models. *IEEE Transactions of ASSP*, 37(12):2091–2110, December 1989.

[4] Peter Steffan, Peter N. Heller, Ramesh A. Gopinath, and C. Sidney Burrus. Theory of regular m-band wavelet bases. *IEEE Transactions on Signal Processing*, 41(12):3497–3511, December 1993.

[5] Martin Vetterli and Cormac Herley. Wavelets and filter banks: Theory and design. *IEEE Transactions on Signal Processing*, 40(9):2207–2232, September 1992.